JOURNAL OF OPTOELECTRONICS AND ADVANCED MATERIALS Vol. 9, No. 1, January 2007, p. 70 - 76

Invited Lecture

Photoluminescence lifetime studies of a-Si:H and a-SiN:H

T. AOKI*, K. IKEDA, N. OHRUI, S. KOBAYASHI, K. SHIMAKAWA[a]
Department of Electronics and Computer Engineering, & Joint Research Center of High-technology, Tokyo Polytechnic University, Atsugi, 243-0297, Japan.
[a] *Department of Electrical and Electronic Engineering, Gifu University, Gifu, 501-1193, Japan.*

We present recent developments in the study of the photoluminescence (PL) lifetime of a-Si:H; in particular, PL excitation (PLE) spectra of singlet- and triplet-excitons and distant-pair (DP) components, and the effects of the defect density on the triple-peak PL lifetime distributions. PLE of the two excitonic components suggests the presence of exciton absorption. Introducing defects significantly quenches the DP components by non-radiative tunneling (NRT) recombination. The lifetime distribution of a-SiN:H obtained by wideband quadrature frequency resolved spectroscopy (QFRS) exhibits a triple-peak structure as well, and its dependences on temperature and generation rate are similar to those of a-Si:H, except for the short-lived lifetime of ~10 ns in a-SiN:H in contrast to that of ~1 μs in a-Si:H. The QFRS study gives spin exchange energy and photon emission rates of the excitons of a-SiN:H.

(Received November 28, 2006; accepted December 21, 2006)

Keywords: a-Si:H, a-SiN$_x$:H, Wideband-QFRS, Exciton, Distant-pair, PLE, Non-radiative tunneling, IR biasing

1. Introduction

Photoluminescence (PL) spectroscopy is one of the more sensitive and non-destructive tools for investigating recombination mechanisms of photoexcited carriers in optoelectronic materials. Particularly, quadrature frequency-resolved spectroscopy (QFRS) of the PL is a powerful technique to measure the widely distributed spectrum of the PL lifetime induced by the disorder of amorphous semiconductors. As reported in a previous paper [1], using a newly developed wideband QFRS technique to analyze the lifetime distribution over almost 11 decades in time (2 ns to 160 s), we found a triple-peak PL lifetime distribution for undoped hydrogenated amorphous Si (a-Si:H) at low temperatures and under the geminate condition, with the photogeneration rate $G \leq 10^{19}$ cm^{-3}s^{-1} as described by Bort et al. [2].

A third lifetime peak τ_D found by our group in the range 0.1–160 s, besides the well-known double lifetime peaks, increases continuously with decreasing G, even far below the geminate condition. This τ_D component reflects the recombination of non-geminate electron-hole (e-h) pairs, i.e., distant-pairs (DPs), in which electrons and holes are separately trapped in the respective band-tails through rapid thermalization after above-bandgap photoexcitation [3]. Thus the observation of the triple-peak lifetime distribution suggests the coexistence of excitonic recombination and DP recombination, even under the geminate condition. At higher temperatures, the distribution becomes a double-peak one, with peaks due to geminate (non-excitonic) and DP recombination [3]. The effect of an external magnetic field on the lifetime distribution also supports the involvement of exciton and DP recombination, under the geminate condition at low temperatures [1].

Meanwhile, light induced electron spin resonance (LESR) signals are generally interpreted as due to photoexcited electron-hole pairs separately trapped into the respective band-tails [2,4,5]. The LESR signal shows a sub-linear G-dependence of the metastable carrier density $n_{met} \propto G^{0.2}$ in the range of G from 10^{15} to 10^{23} cm^{-3}s^{-1} and the residual LESR signal continues to decay over 10^4s after turning off the excitation light. However, the metastable carrier density obtained from the QFRS of the PL is linearly dependent on G under geminate conditions $G \leq 10^{19}$ cm^{-3}s^{-1}, and residual PL decay has not been observed at times longer than 10 s, except by an indirect method using infrared (IR) superposition as a probe [6].

We have discovered, however, that the third lifetime peak τ_D increases continuously with decreasing G even far below the geminate condition, and shows a sub-linear dependence of the metastable carrier density $n_D = \eta_D G \tau_D \propto G^{0.2}$, where η_D is a quantum efficiency for the DP component deduced by deconvoluting QFRS spectra. This agrees with the G-dependence of the light induced electron spin resonance (LESR) signals [3]. Automatically varying the time-constant of the lock-in detection of the residual PL after cessation of the PL excitation light, we have observed the PL decay over 10^4 s and demonstrated that the integration of the PL decay depends on G as $\propto G^{0.2}$ [7]. Thus, we have solved the long standing open questions concerning the discrepancies of the G-dependence and the residual decay between LESR and PL in a-Si:H [3,7,8].

Following our previous paper [1], we shall present here a further development of PL lifetime studies of a-Si:H; effects of the PL excitation energy (PLE), defect density and infrared (IR) biasing on the triple-peak QFRS

spectra. The PL lifetime distribution of a-SiN:H is studied by wide-band QFRS, exhibiting a triple-peak structure with a short-lived lifetime peak at τ_S of ~10 ns, in contrast to that of ~1 μs in a-Si:H.

2. Experimental

All the films of a-Si:H and a-SiN_x:H for PL measurements were deposited on roughened Al substrates by VHF plasma CVD (Chemical Vapor Deposition) with a novel impedance matching method [9]; a-Si:H films of thickness 0.9 – 1.1 μm with various defect densities were obtained mainly by varying the substrate temperatures at a frequency of 50 MHz. The defect densities of the a-Si:H films were determined by CPM (Constant Photocurrent Method) spectroscopy. Films of a-SiN_x:H were produced from a mixture of SiH_4 and N_2 gases at a substrate temperature of 350 °C, at frequencies of 50 – 150 MHz and power densities of 35 – 280 $mWcm^{-2}$. The optical bandgap E_{opt} was determined from Tauc plots obtained by fiber-optic- transmission measurements using a Perkin-Elmer Lambda 900 spectrophotometer at 3.7 K. The Urbach tail energy E_U was also obtained from the optical transmission spectrum at room temperature. In addition to these data, the nitrogen content x determined from transmission spectra using a JOEL Winspec 100 FTIR (Fourier Transform Infrared) spectrophotometer and with a thickness d obtained using a SCI Filmtek 2000 fiber-optic-spectrophotometer are tabulated for the five samples of a-SiN_x:H in Table 1.

Table.1 x; nitrogen content, E_{opt}; optical bandgap, E_U; Urbach tail energy, d; thickness, I_{PL}; PL intensity, E_{PLS}; PL peak energy of the singlet exciton component, E_{PLT}; PL peak energy of the triplet exciton component, E_{ex}; exchange energy, τ_S; singlet exciton lifetime, τ_T; triplet exciton lifetime, η_S/η_T; QE ratio of the singlet- to triplet - exiciton components for the five a-SiN_x:H samples.

Sample No.	SN01	SN02	SN03	SN04	SN05
x (a-SiN_x:H)	0.49	0.84	1.14	1.18	1.43
E_{opt} (3.7K)	2.07	2.47	2.67	2.89	3.04
E_U [eV]	0.12	0.22	0.34	0.29	0.36
d [μm]	1.52	2.43	2.29	1.54	8.34
I_{PL} [a.u.]	0.3	0.5	4	1	6
E_{PLS} [eV]	1.30	1.96	2.00	1.99	2.15
E_{PLT} [eV]	1.25	1.78	1.82	1.82	1.97
E_{ex} [eV]	0.05	0.18	0.18	0.17	0.18
τ_S [ns]	10	5.0	10	6.1	13
τ_T [ms]	0.5	0.6	2.0	1.0	2.0
η_S/η_T	2.3	4.9	4.8	5.9	3.9

The PL of a-Si:H was excited mainly at 2.33 eV, and PL excitation spectroscopy (PLE) was measured by eight semiconductor lasers with emission energies E_X ranging from 1.46 to 1.94 eV. The PL of a-SiN:H was excited by laser light of E_X = 2.33, 2.61, 3.04 and 3.31 eV. The spectrally integrated or dispersed PL was detected by an infrared (IR) photomultiplier tube (PMT; R5509-42, Hamamatsu) at photon energies ≥ 0.89 eV. The PL intensity I_{PL} of the a-SiN_x:H samples in Table 1 is the dc photocurrent (arbitrary units) of the PMT detecting spectrally integrated PL, excited at E_X = 3.31 eV and 13 K.

PL lifetime distributions were measured by the wideband QFRS technique, measurable over almost 11 decades of lifetime from 2 ns to 160 s, as previously reported [1]. The effects of IR on the QFRS spectra of a-Si:H were studied by employing the wideband QFRS for the PL excited with above-bandgap radiation E_X = 2.33 eV in superposition with sub-bandgap light of 0.37 eV (3.39 μm) IR laser, with an irradiation intensity of 75 $mWcm^{-2}$, corresponding to 1.3×10^{18} photons·$cm^{-2}s^{-1}$.

3. Results and discussion

3.1. a-Si:H

Figure 1(a) shows the triple-peak QFRS spectra, at various excitation energies E_X and 3.7 K, for the spectrally integrated PL of a high-quality a-Si:H film having a defect density $N_d \approx 1.4 \times 10^{16}$ cm^{-3} and a thickness of 9.3 μm; each spectrum has three lifetimes peaks at τ_S (~μs), τ_T (~ms) and τ_D well below the geminate condition of $G = 2.0 \times 10^{15}$ $cm^{-3}s^{-1}$. The peaks at τ_S and τ_T are the well-known double peaks [10] while the peak at the longest lifetime τ_D is the third one discovered by our group [3]. The quantum efficiency (QE) η_D, proportional to the area of the third τ_D component, is larger and τ_D is longer at higher E_X. This is a result of DP recombination because photo-excited carriers tend to diffuse apart rather than form a geminate pair or an exciton during thermalization at a photoexcitation energy E_X well above the mobility gap [1,3]. PLE spectra for the three components, i.e., the QEs η_S, η_T and η_D plotted as functions of E_X, are shown in Fig.1(b), where the QEs were determined by deconvoluting the QFRS spectra of Fig.1(a). Both the QEs η_S and η_T are larger than η_D in the range of E_X from 1.5 to 1.7 eV.

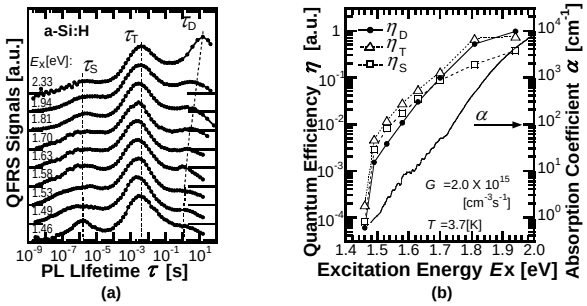

Fig. 1 (a) QFRS spectra of high-quality a-Si:H for various excitation energies E_X at $G = 2.0 \times 10^{15} cm^{-3}s^{-1}$ and 3.7 K. (b) Quantum efficiencies (QEs) of (□)η_S, (Δ)η_T and (●)η_D of the three lifetime components τ_S, τ_T and τ_D, respectively, as functions of E_X, and an absorption spectrum (α) obtained at 3.7 K.

A self-trapped-exciton (STE), composed of an electron bound to a self-trapped hole (STH), is responsible for the former two components, having PL peak energies around at ~1.3 eV [1,8]. If these higher absorption coefficients of the two components are assumed to be the exciton absorptions, the energy difference between the excitonic absorption energy and the PL peak energy amounts to ~ 0.2 – 0.4 eV, which coincides with the STH trapping energies of 0.24 – 0.35 eV [11]. The Coulomb binding energy of the electron bound to the STH was estimated to be ~5 meV [8] and the singlet-triplet exchange energy E_{ex} was determined from the difference between the PL peak energies of the τ_S and τ_T components, being ~40 meV [12]. Thus we shall introduce the excitonic recombination model as shown in Fig. 2.

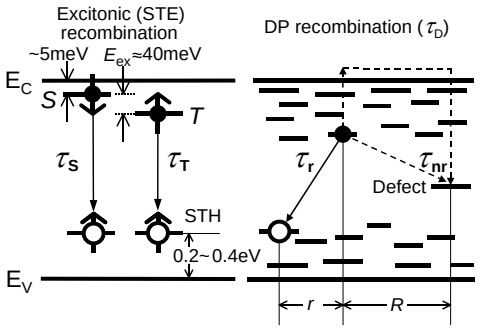

Fig. 2. Recombination model of a-Si:H. consisting of singlet (τ_S) and triplet (τ_T) self-trapped excitons (STE) and a distant-pair (DP(τ_D)) with e-h pair separation r. The exchange energy $E_{ex} \approx 40$ meV and singlet-exciton binding energy ~5 meV are obtained in Refs. [8] and [12] respectively. The electron of the DP has a distance R to a defect. The thin solid arrows indicate radiative recombination. An oblique dotted arrow indicates non-radiative tunneling and a vertical one to the defect indicates non-competing non-radiative recombination. The thick arrows indicate the spins of electrons and holes.

In addition, the PLE spectrum of the τ_D component declines faster into the bandgap than those of the τ_S and τ_T components, while the PL peak energy of the τ_D component is the lowest [1,8]. This is a manifestation of the largest Stokes shift of the τ_D component, which presumably results from the recombination of DPs deeply trapped in tail states in Fig.2.

Figure 3(a) demonstrates how the triple-peak QFRS spectra change as the defect density N_d increases. The deconvoluted QFRS spectra show little change of the lifetimes τ_S and τ_T with increase of N_d, in contrast to the decrease of the QEs η_S and η_T. This was interpreted as non-competing non-radiative recombination (NRR) introduced by the defects, where photoexcited carriers are rapidly captured by the defects, usually within 10^{-12} s, during the thermalization process from extended or higher tail states after PL excitation [13].

On the other hand, however, the lifetime of the third longest-lived component $\tau_D \geq 0.1$ obviously decreases as the QE decreases with increase of N_d in Fig. 3(a), and the logarithmic plot of η_D with arbitrary unit against N_d coincides with that of τ_D in Fig. 3(b). This indicates that the DP radiative recombination competes with the NRR introduced by the defects. At a low temperature, electrons and holes are localized and immobile in the respective band-tails [7]. Both the radiative and non-radiative transitions must therefore involve tunneling, as shown in Fig. 2; a tunneling distance for radiative tunneling (RT) recombination is an e-h DP separation r, and that of the non-radiative tunneling (NRT) recombination is a distance R between an electron and a defect, when the electron is assumed to be the particle which tunnels to the defect.

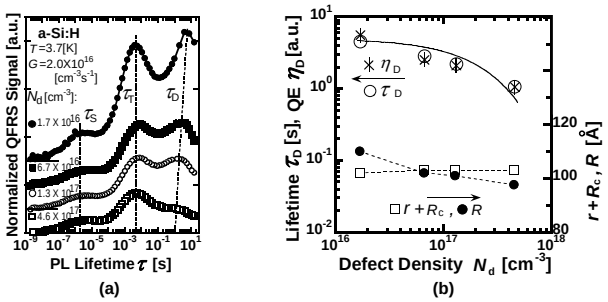

Fig. 3. (a) QFRS spectra of a-Si:H samples with defect densities $N_d = 1.7 \times 10^{16}$, 6.7×10^{16}, 1.3×10^{17} and 4.6×10^{17} cm^{-3}. (b) (○) the DP lifetime τ_D and (*) QE η_D obtained from (a) against N_d. The solid curve is derived from Street's model [14]. Also (□) the e-h separation $r + R_c$ and (●) the distance R between the electron and defect plotted against N_d. Critical length $R_c = (a/2)\ln(\nu_0\tau_0) \approx 32$ Å with $a = 7$ Å, $\nu_0 = 10^{12}$ s^{-1} and $\tau_0 = 10^{-8}$ s.

The model of Street et al. [14], in which all electrons trapped in band-tail states within a critical radius R_d of a dangling bond are assumed to tunnel to the defect and recombine non-radiatively, predicts the reduction of QE by a factor of $\exp(-4\pi R_d^3 N_d/3)$. Setting $R_d = 100$ Å, we can fit the factor to the QE η_D as shown by a solid curve in Fig. 3(b). When NRT with a lifetime τ_{nr} is competing with RT recombination with a lifetime τ_r, the actual lifetime τ_D and the QE η_D are given by,

$$\tau_D^{-1} = \tau_r^{-1} + \tau_{nr}^{-1} \quad (1)$$

and

$$\eta_D = \tau_r^{-1}/(\tau_r^{-1} + \tau_{nr}^{-1}) = \tau_D/\tau_r. \quad (2)$$

The RT lifetime τ_r is expressed as

$$\tau_r = \tau_0 \exp(2r/a), \quad (3)$$

where τ_0, and a are the dipole transition time usually ~10^{-8} s and the electron localization radius, respectively. The NRT lifetime τ_{nr} is given by

$$\tau_{nr} = \nu_0^{-1} \exp(2R/a), \quad (4)$$

with ν_0 having a typical phonon frequency ~10^{12} s^{-1}.

Both τ_r and τ_{nr} are determined from the data of τ_D and η_D, using the eqs. (1) and (2). Since $\eta_D \propto \tau_D$ in Fig. 3(b), τ_r is independent of N_d but τ_{nr} decreases with an increase in N_d. The RT recombination prevails over the competing NRT recombination, or vice versa, depending upon whether $\tau_r^{-1} > \tau_{nr}^{-1}$ or $\tau_r^{-1} < \tau_{nr}^{-1}$, which corresponds to $R > r + R_c$ or $R < r + R_c$ with a critical length $R_c = (a/2)\ln(\nu_0 \tau_0)$, deduced from eqs. (3) and (4). For each defect density, N_d, $r + R_c$ and R were determined from τ_r and τ_{nr}, using eqs. (3) and (4), respectively. The electron localization radius a was assumed to be 7 Å, so that R averages R_d = 100 Å approximately, which gives $R_c \approx 30$ Å. As N_d increases, the DP separation r is almost constant, but R decreases by ~10 Å and $R < r + R_c$ holds for defective samples with $N_d \geq 6.7 \times 10^{16}$ cm^{-3}, indicating the dominance of NRT over RT.

The QFRS spectra of the defect-rich sample with $N_d = 4.6 \times 10^{17}$ cm^{-3} are demonstrated in Fig. 4 (a) for various G. In particular, the τ_D component decreases in both lifetime and area below $G = 1.6 \times 10^{15}$ $cm^{-3}s^{-1}$. The lifetimes τ_D and QEs η_D of the high-quality sample with $N_d = 1.7 \times 10^{16}$ cm^{-3} and the defect-rich sample are shown in Fig. 4(b) as functions of G. The lifetime τ_D of the high-quality sample monotonically increases up to 64 s with decreasing G to 9.0×10^{14} $cm^{-3}s^{-1}$, but that of the defect-rich sample has a peak at $G = 1.6 \times 10^{15}$ $cm^{-3}s^{-1}$. Such a singular phenomenon of the defect-rich sample arises because the metastable carrier density is so much smaller than N_d at the very low G that the NRT at the defect sites prevails over RT and participates in shortening the fate of the metastable carriers [7,15].

In Fig. 4(c), as functions of G, we plot τ_r of both the samples and τ_{nr} of the defect-rich sample determined from τ_D and η_D, by using eqs. (1) and (2). Individual points of τ_r lie in a straight line vs. $G^{-0.8}$, showing that the radiative recombination approximately obeys the DP theory even for the defect-rich sample. Moreover, the NRT lifetime τ_{nr} almost lies on the $G^{-0.8}$ line, which indicates that both the DP separation r and the distance from the electron to the defect R are dependent on G (Fig. 4(c)). Fig. 4 (c) also shows that $R < r + R_C$ holds over the whole range of G for the defect-rich sample, where the NRT dominates over the radiative DP recombination.

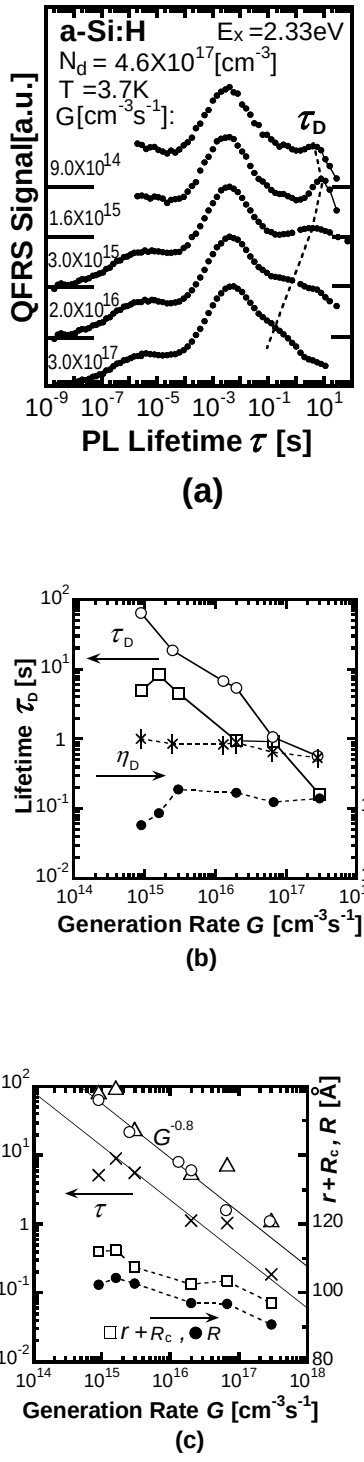

Fig. 4. (a) QFRS spectra of the defect-rich a-Si:H with $N_d = 4.6 \times 10^{17}$ cm^{-3} for various G. (b) (○) the lifetime τ_D and (∗) QE η_D as functions of G for the high-quality sample with $N_d = 1.7 \times 10^{16}$ cm^{-3}. (□) τ_D and (•) η_D for the defect-rich sample. (c) The radiative lifetimes τ_r for (○) the high-quality and (Δ) the defect-rich samples, and (×) non-radiative lifetimes τ_{nr}, (□) r + Rc, (•)R for the defect-rich sample, as functions of G.

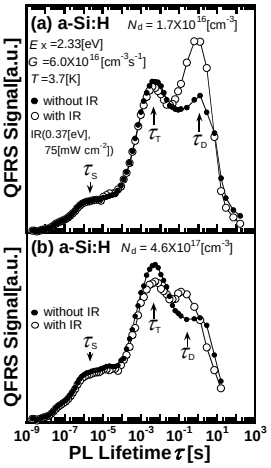

Fig. 5. (a) QFRS spectra of the high-quality a-Si:H sample (○) with and (●) without IR biasing of 0.37 eV and 75 mWcm^{-2}. (b) The same as (a) except for the defect-rich a-Si:H sample.

Figs. 5(a) and (b) demonstrate the QFRS spectra excited at 3.7 K, E_X = 2.33 eV and $G = 6.0 \times 10^{16}$ cm^{-3}s^{-1} (well below the geminate condition) with and without IR superposition for the high quality sample and the defect-rich sample, respectively. The IR biasing enhances the DP component of the high-quality film but shortens the lifetime peak τ_D and its skirt on a logarithmic lifetime scale (Fig. 5(a)). Deconvolution of the spectra gives τ_D = 1.20 s and η_D = 0.40 without IR and τ_D = 0.90 s and η_D = 0.54 with IR, from which the metastable carrier density of the τ_D component $n_D = \eta_D G \tau_D$ amounts to 2.9×10^{16} cm^{-3} regardless of IR biasing. On the other hand, IR biasing of the defect-rich sample significantly shortens τ_D from 1.25 s to 0.31 s whereas η_D slightly increases from 0.12 to 0.17, thereby reducing n_D from 0.9×10^{16} cm^{-3} to 0.3×10^{16} cm^{-3} (Fig. 5(b)).

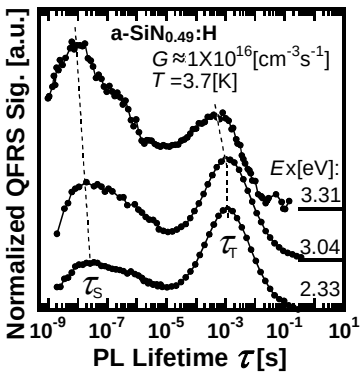

Fig. 6 Temperature evolution of the QFRS spectra for the a-SiN$_{0.49}$:H SN01 sample at E_X = 2.33 eV and $G \approx 1 \times 10^{17}$ cm^{-3}s^{-1}. A new hump (τ_G), which appears above 60 K, is attributed to non-excitonic but geminate recombination. A very small hump (in the inset) in the lifetime range from 1 - 10 s is the DP recombination Component.

By employing the DP recombination model in Fig.2, the results are interpreted in terms of the IR-induced release of deeply trapped photocarriers; in other words, metastable carriers from localization in the band-tail states. The IR superposition activates an immobile carrier, e.g., an electron localized in a conduction band-tail state at low temperature, which makes a hop-up to an unoccupied and higher energy tail state or extended state. Since the density of localized states is larger for the higher energy state, the activated electron will diffuse to a tail state closer to either a hole or a defect, i.e., shorten either r or R. If the electron is activated to the extended states and diffuses, the shortening of either r or R will be more pronounced. However, when non-radiative centers such as defects are negligible, so that R is not affected by the IR and the inequality $R > r + R_c$ always holds, all the carriers thus excited into the higher tail-states by IR will recombine radiatively and shorten τ_D, due to the decrease in r. Even though the electron is activated to the extended states and diffuses, it is recaptured by a tail state and then recombines radiatively. Hence, the metastable carrier density is scarcely affected by the IR superposition in the high-quality sample.

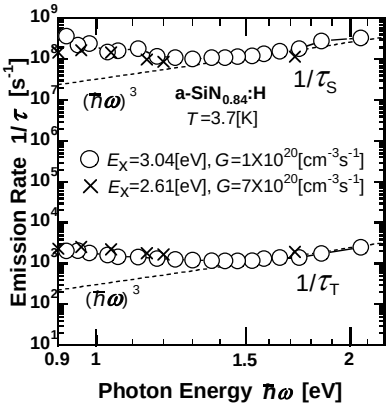

Fig. 7. Excitation energy (E_X) dependence of QFRS spectra of the a-SiN$_{0.49}$:H SN01 sample.

When NRT is not negligible, a metastable carrier, e.g., an electron activated to the higher tail-states by IR biasing, will make a transition to a tail state closer to either a hole or a competing NRT center. This results in a shortening of the distance R between the electron and defect as well as r. Furthermore, when the carrier is excited to the extended states, it diffuses to either a closer hole to recombine radiatively or to a closer defect which acts as a non-competing NRR center. Thus, the IR superposition during QFRS reduces n_D as well as τ_D in the defect-rich sample. A slight decrease of the two excitonic components induced by IR biasing in Fig. 5(b) is explained as follows; the IR radiation releases electrons and holes from excitons into the respective extended states. Some of these carriers are recaptured as excitons, and others recombine via non-competing NRR centers, thereby decreasing the excitonic components [16].

3.2. a-SiN$_x$:H

Fig. 6 shows the temperature evolution of the QFRS spectra of the a-SiN:H sample *SN01* at $G \approx 1 \times 10^{17}$ cm^{-3}s^{-1} and E_X = 2.33 eV. The QFRS spectrum at the lowest temperature 3.7 K shows the triple-peak lifetime distribution where the short-lived lifetime peak τ_S falls to ~10 ns, in contrast to that of ~1 μs for a-Si:H. The ns component was also observed by Ogihawa et al. [17] using pulsed PL excitation. It is reasonable to attribute the short-lived component to the emission from singlet-exciton recombination, i.e., the fluorescence, which commonly has a lifetime of ~10 ns or less in luminescent condensed matter. This suggests that the singlet-exciton is involved in the short-lived component of the double peak lifetime distributions of a-Si:H and other amorphous semiconductors, of which the rather longer lifetime is interpreted by the STE [12]. At the elevated temperature of 60 K, there appears a small peak around at ~10 μs between τ_S and τ_T as observed in a-Si:H, which is due to the recombination of geminate pairs prevented from forming excitons [3]. We can recognize a small peak due to the DP recombination at 3.7 K and the long lifetime 1–10 s.

The excitation energy (E_X) dependence of the same sample is shown in Fig. 7; the lifetime peaks τ_S and τ_T slightly shorten and the QE ratio of the short- to long-lived component η_S/η_T increases as E_X increases at 3.7 K and $G \approx 1 \times 10^{16}$ cm^{-3}s^{-1}. The latter was also observed in g-As_2S_3 and a-Se, having rather large singlet-triplet exchange energies $E_{ex} \approx 0.10$ and 0.16 eV respectively, and explained by the exciton model [18,19]. Namely, as the singlet state is higher than the triplet state by E_{ex}, the singlet states are more populated under higher E_X at low temperatures, thereby enhancing the τ_S component.

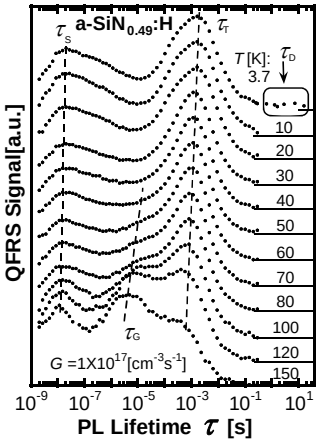

Fig. 8. (a) QFRS spectra of the a-SiN$_{0.84}$:H SN02 sample. The inset shows the DP component taken at various G. (b) (□) the lifetime τ_D, (●) QE η_D and (○) radiative recombination lifetime τ_r deduced from τ_D/η_D as functions of G for the SN02 sample.

Fig. 8(a) demonstrates the QFRS spectrum of the a-SiN:H sample *SN02* at 3.7 K, E_X = 3.04 eV and $G = 1.0 \times 10^{19}$ cm^{-3}s^{-1} and the inset is the τ_D components for various generation rates G. The spectra have clear triple-peaked structures with τ_D depending on G. The dependences of τ_D, η_D and $\tau_r = \tau_D/\eta_D$ on G are plotted in Fig. 8(b), where τ_r begins to decrease in proportion to $G^{-0.8}$ as G increases from 9.7×10^{19} cm^{-3}s^{-1}. The deviation of τ_r from the $G^{-0.8}$ line below $G = 1.0 \times 10^{19}$ cm^{-3}s^{-1} can be interpreted by the effect of defects, as above-mentioned for the defect-rich a-Si:H sample in Fig. 4(a). However, here G is unusually large compared to that for the defect-rich a-Si:H. This is presumably due to the larger defect density of the a-SiN:H sample. The maximum ratio of the QE $\eta_D/(\eta_S + \eta_T)$ is ~0.02 for the a-SiN:H sample *SN02* at $G = 9.7 \times 10^{19}$ cm^{-3}s^{-1} and ~0.67 for the defect-rich a-Si:H sample of Fig. 4(a) at $G = 3.0 \times 10^{15}$ cm^{-3}s^{-1}, which suggests that the a-SiN:H *SN02* sample is highly defective compared with the defect-rich a-Si:H sample with $N_d = 4.6 \times 10^{17}$ cm^{-3}. This is also supported by the small ratio of the PL intensity for a-SiN:H *SN02* to that of the defect-rich a-Si:H sample, being ~0.12 at 3.7 K in spite of the different E_X.

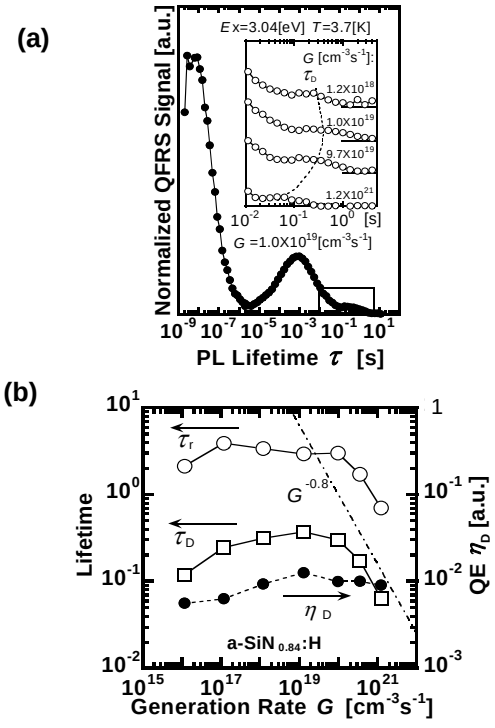

Fig. 9 Emission rates ($1/\tau$) for singlet- and triplet-exciton recombination vs. PL photon energy $\hbar\omega$ plotted on a double-logarithmic scale for the SN02 sample at (×) E_X = 2.61eV, $G \approx 7 \times 10^{20}$ cm^{-3}s^{-1} and (○) E_X = 3.04 eV, $G \approx 1 \times 10^{20}$ cm

The recombination rates $1/\tau_S$ and $1/\tau_T$, as functions of PL photon energy $\hbar\omega$, are deduced from the lifetime peaks of the $\hbar\omega$-evolved QFRS spectra of the PL dispersed by a monochromator for the sample *SN02*, as shown in Fig. 9. This also supports the suggestion of excitonic emission for the τ_S and τ_T components, since both the emission rates depend on $\hbar\omega$ in proportion to $(\hbar\omega)^3$ for $\hbar\omega$ higher than ~1.4 eV [12]. Deviations of $1/\tau_S$ and $1/\tau_T$ from the $(\hbar\omega)^3$ law for $\hbar\omega$ below 1.4 eV are presumably due to defect luminescence, as observed in a-Si:H in the region 0.7 – 0.9 eV [14], since the PMT, sensitive to $\hbar\omega \geq 0.89$ eV, may detect radiative recombination from the defect luminescence of a-SiN:H. We have recorded the PL spectra of the QFRS signal by fixing the PL modulation frequencies corresponding to τ_S and τ_T, i.e., the approximate PL spectra of the two components discriminated by lifetimes τ_S and τ_T, which resemble each other in spectral shape but differ in PL peak energy E_{PL} by the spin exchange energy of singlet- and triplet-excitons $E_{ex} \geq 0.05$ eV [1,8]. The PL peak energies E_{PLS} and E_{PLT} for the τ_S and τ_T components, respectively and E_{ex} are listed in the table 1. It should be noted that E_{ex} ~0.05 eV of *SN01* with a small nitrogen content of $x = 0.49$ is close to that of a-Si:H ~ 0.04 eV [12], but it increases to 0.18 eV and keeps almost constant for the samples with $x = 0.89 – 1.43$.

4. Conclusions

The PLE of the two excitonic components discriminated from QFRS spectra of high-quality a-Si:H films at a low temperature indicates the excitonic absorption in the photon energy range from 1.5 eV to 1.7 eV. Significant quenching of the DP components upon increasing the defect density indicates that NRT recombination at defect sites competes with the RT recombination of DPs. The effects of IR biasing on the QFRS were found to be noticeable for the DP component of the defect-rich a-Si:H film. In particular, IR promotes localized carriers to recombine through both competing NRT and non-competing NRR at the defect sites.

The PL of a-SiN:H films was also found to show triple-peaked QFRS spectra and support the three recombination mechanisms, i.e., the two excitonic and the DP recombination. The a-SiN:H films possess normal fluorescence lifetimes, supporting the universal involvement of the singlet-exciton in amorphous semiconductors. The DP component of a-SiN:H is very small compared with that of even defective a-Si:H films, due to the higher defect density. It should be noticed that the exchange energy E_{ex} is close to that of a-Si:H for a-SiN_x:H with a low nitrogen content $x = 0.49$, but keeps constant at ~ 0.18 eV for $x \geq 0.89$.

Acknowledgements

The work was financially supported in part by the Japan Private School Promotion Foundation. One of the authors, T.A. would like to express his gratitude to Professor W. Fuhs for suggesting effects of non-radiative recombination on the PL lifetime distributions.

References

[1] T. Aoki, T. Shimizu, D. Saito, K. Ikeda, J. Optoelectron. Adv. Mater. **7**, 137 (2005).
[2] M. Bort, W. Fuhs, S. Liedtke, R. Stachowitz, R. Carius, Philos. Mag. Lett. **64**, 227 (1991).
[3] T. Aoki, T. Shimizu, S. Komedoori, S. Kobayashi, K. Shimakawa, J. Non-Cryst. Solids **338-340**, 456 (2004).
[4] F. Boulitrop and D. J. Dunstan, Solid State Commun. **44**, 841 (1982).
[5] B. Yan, N. A. Schlutz, A. L. Efros, P. C. Taylor, Phys. Rev. Lett. **84**, 4180 (2000).
[6] R. Carius, W. Fuhs, A. Schrimpf, Tetrahedrally Bonded Amorphous Semiconductors, ed. D. Adler and H. Fritzsche, Plenum Press, NY. (1985), p.366.
[7] T. Aoki, K. Ikeda, S. Kobayashi, K. Shimakawa, Philos. Mag. Lett. **86**, 137 (2006).
[8] T. Aoki, J. Non-Cryst. Solid **352**, 1138 (2006).
[9] T. Aoki, K. Fukasawa, Y. Nishikawa, N. Mikoshiba, Jpn. J. Appl. Phys. **35**, 4799 (1996).
[10] F. Boulitrop, D. J. Dunstan, J. Non-Cryst. Solid **77-78**, 663 (1985).
[11] I. Hirabayashi, K. Morigaki, Philos. Mag. B **54**, L119 (1986).
[12] T. Aoki, J. Mat. Sci. Mat. Electron **14**, 697 (2003).
[13] M. Bort, R. Carius, W. Fuhs, J. Non-Cryst. Solids **114**, 280 (1989).
[14] R. A. Street, Hydrogenated Amorphous Silicon, Cambridge University Press, Cambridge (1991).
[15] R. I. Shklovskii, E. I. Levin, H. Fritzsche, S. D. Baranovskii, Transport, Correlation and Structural Defects Vol. **3**, ed. H. Fritzsche, World Scientific Singapore (1990), p.161.
[16] O. Rubel, S. D. Baranovskii, K. Hantke, B. Kunert, W. W. Rühle, P. Thomas, K. Volz, W. Stolz, Phys. Rev. B **73**, 233201 (2006).
[17] C. Ogihara, H. Takemura, H. Yoshida, K. Morigaki, J. Non-Cryst. Solids **266-269**, 574 (2000).
[18] T. Aoki, S. Komedoori, S. Kobayashi, T. Shimizu, A. Ganjoo, K. Shimakawa, J. Non-Cryst. Solids **326-327**, 273 (2003).
[19] T. Aoki, D. Saito, K. Ikeda, S. Kobayashi, K. Shimakawa, J. Optoelectron. Adv. Mater. **7**, 1749 (2005).

*Corresponding author:aoki@ee.t-kougei.ac.jp